136822-75-8; **2d**, 136822-76-9; **3a**, 136838-18-1; **3b**, 136838-19-2; **3c**, 136838-20-5; **3d**, 136856-86-5; **3e**, 136838-22-7; $Ru_2Cl(O_2CMe)_4$, 38833-34-0.

Supplementary Material Available: For $Ru_2(OH_2)Cl(MeCN)(O_2CC_6H_4$-*p*-$OMe)_4(PPh_3)_2$ (**2b**) and $Ru_2(OH_2)(MeCN)_2(O_2CC_6H_4$-*p*-$NO_2)_4(PPh_3)_2 \cdot 1.5CH_2Cl_2$ (**3e**), details of crystal structure determination, tables of crystal data, positional and isotropic thermal parameters, anisotropic thermal parameters, and bond lengths and angles (22 pages); tables of observed and calculated structure factors for **2b** and **3e** (70 pages). Ordering information is given on any current masthead page.

Contribution from the Department of Chemistry, Purdue University, West Lafayette, Indiana 47907

Reactions of the Polyhydride Complex $ReH_7(PPh_3)_2$ with Hydroxypyridine and Mercaptopyridine Ligands. Formation of Hydrido Complexes of Rhenium(III), Rhenium(IV), and Rhenium(V) and the Characterization of Eight-Coordinate Isomers in the Solid State and in Solution

Malee Leeaphon, Phillip E. Fanwick, and Richard A. Walton*

Received August 30, 1991

The reactions of the heptahydride complex $ReH_7(PPh_3)_2$ with 2-hydroxypyridine (Hhp), 2-mercaptopyridine (Hmp) and 2-hydroxy-6-methylpyridine (Hmhp) in acetone afford the diamagnetic seven-coordinate complexes $ReH(L)_2(PPh_3)_2$ (L = hp, mp, mhp), which can be oxidized by one electron when treated with $[(\eta^5\text{-}C_5H_5)_2Fe]PF_6$ in dichloromethane to give paramagnetic $[ReH(L)_2(PPh_3)_2]PF_6$. These are rare examples of mononuclear rhenium(IV) hydrides. While the 17-electron mp derivative is stable in solution, the related hp and mhp complexes decompose (probably by a disproportionation mechanism) to give the dihydrides $[ReH_2(L)_2(PPh_3)_2]PF_6$ as the major products. In these latter reactions small quantities of the seven-coordinate oxorhenium(V) complexes $[ReO(L)_2(PPh_3)_2]PF_6$ can also be isolated. The crystal structure of $[ReO(mhp)_2(PPh_3)_2]PF_6 \cdot C_2H_4Cl_2$ (**4**) shows that it is based upon a distorted pentagonal bipyramid with a P-Re-P angle of ca. 169° and with the oxo ligand occupying a position within the pentagonal plane. The diamagnetic dihydrido species $[ReH_2(L)_2(PPh_3)_2]PF_6$ are also formed in all cases upon treatment of $ReH(L)_2(PPh_3)_2$ with HPF_6 in dichloromethane. The mp derivative is unstable and converts to $[ReH(mp)_2(PPh_3)_2]PF_6$ with loss of H_2. The hp complex $[ReH_2(hp)_2(PPh_3)_2]PF_6$ is stable both in the solid state and in solution, and is identical in all respects with the form of this complex that is isolated from the decomposition of $[ReH(hp)_2(PPh_3)_2]PF_6$. On the other hand, the complex of composition $[ReH_2(mhp)_2(PPh_3)_2]PF_6$ exists in two geometric isomeric forms. The product that is obtained upon decomposition of the 17-electron complex $[ReH(mhp)_2(PPh_3)_2]PF_6$ is denoted as the cis isomer and is the more thermodynamically stable form of the two. The trans isomer is the form that is obtained by protonation of neutral $ReH(mhp)_2(PPh_3)_2$. Both isomers have structures that are based upon distorted dodecahedral geometries with the hydrogen and oxygen atoms at the A sites and the nitrogen and phosphorus atoms at the B sites of an MA_4B_4 dodecahedron. Crystal structures on one form of the trans isomer and two different crystalline forms of the cis isomer have been determined, viz., *trans*-$[ReH_2(mhp)_2(PPh_3)_2]PF_6 \cdot C_2H_4Cl_2$ (**1**), *cis*-$[ReH_2(mhp)_2(PPh_3)_2]PF_6 \cdot (CH_3)_2CO$ (**2**), and *cis*-$[ReH_2(mhp)_2(PPh_3)_2]PF_6 \cdot 0.5C_2H_4Cl_2$ (**3**). Each isomer appears to be a classical dihydride. They both have an independent existence in solution although the trans isomer converts very slowly to the cis isomer. This is the first time that eight-coordinate geometric isomers which are stable both in the solid state and in solution have been structurally characterized. These two isomers, as well as $[ReH_2(hp)_2(PPh_3)_2]PF_6$, are easily deprotonated by NEt_3 and/or DBU to re-form the parent neutral monohydrides $ReH(L)_2(PPh_3)_2$. Crystal data for **1** (−62 °C): triclinic space group $P\bar{1}$ (No. 2), a = 13.382 (2) Å, b = 13.723 (2) Å, c = 15.593 (2) Å, α = 107.06 (1)°, β = 96.54 (1)°, γ = 114.05 (1)°, V = 2408 (2) Å^3, Z = 2. Crystal data for **2** (−96 °C): orthorhombic space group *Pbca* (No. 61), a = 19.292 (2) Å, b = 22.399 (2) Å, c = 22.314 (2) Å, $\alpha = \beta = \gamma$ = 90°, V = 9642 (3) Å^3, Z = 8. Crystal data for **3** (+20 °C): triclinic space group $P\bar{1}$ (No. 2), a = 15.075 (4) Å, b = 18.640 (4) Å, c = 20.662 (6) Å, α = 114.53 (1)°, β = 100.44 (2)°, γ = 98.40 (2)°, V = 5033 (5) Å^3, Z = 4. Crystal data for **4** (+20 °C): monoclinic space group $P2_1/c$ (No. 14), a = 11.794 (2) Å, b = 14.168 (1) Å, c = 31.359 (5) Å, β = 110.776 (6)°, V = 4899 (2) Å^3, Z = 4. All structures were refined by full-matrix least-squares methods to the following values of R (R_w given in parentheses) for the stated number of data with $I > 3.0\sigma(I)$: **1**, 0.023 (0.030), 5706 data; **2**, 0.036 (0.049), 4536 data; **3**, 0.059 (0.081), 8473 data; **4**, 0.041 (0.049), 4525 data.

Introduction

Transition-metal polyhydrides are well-known for exhibiting fluxionally.[1] This is especially true in the case of rhenium polyhydrides, for which a greater variety of such complexes exist than for any other transition metal.[2] Accordingly, one would not normally expect geometric isomerism to be encountered in solutions of such species, especially for those compounds that possess coordination numbers greater than 6. Indeed, the phenomenon of geometric isomerism is rarely encountered in the case of eight-coordination, and the definitive structural characterization of such isomers has only been reported in rare instances for solid-state species.[3,4] and in no instance in solution. Nonetheless, while the stabilization of eight-coordinate geometric isomers has long been recognized as a challenging and somewhat daunting task,[5] a series of important studies in the period 1977-1985 by Archer and Donahue[6] on tungsten(IV) complexes that contained four bidentate or two tetradentate donors showed that eight-co-

(1) See, for example: Hlatky, G. G.; Crabtree, R. H. *Coord. Chem. Rev.* **1985**, *65*, 1 and references contained therein.
(2) Conner, K. A.; Walton, R. A. In *Comprehensive Coordination Chemistry*; Pergamon: Oxford, England, 1987; Chapter 43, pp 125-213.
(3) (a) Sen, A.; Chebolu, V.; Rheingold, A. L. *Inorg. Chem.* **1987**, *26*, 1821. (b) Chebolu, V.; Whittle, R. R.; Sen, A. *Inorg. Chem.* **1985**, *24*, 3082. (c) Fanfani, L.; Nunzi, A.; Zanazi, P. F.; Zanzari, A. R. *Acta Crystallogr., Sect. B: Struct. Crystallogr. Cryst. Chem.* **1972**, *28*, 1298.
(4) Isomers can also be obtained by varying a counterion as, for example, in the case of salts of the $[Nb(C_2O_4)_4]^{4-}$ anion, viz., $K_2(H_3NCH_2CH_2NH_3)[Nb(C_2O_4)_4] \cdot 4H_2O$ and $K_4[Nb(C_2O_4)_4] \cdot 3H_2O$. See: Cotton, F. A.; Diebold, M. P.; Roth, W. J. *Inorg. Chem.* **1987**, *26*, 2889.
(5) Lippard, S. J. *Prog. Inorg. Chem.* **1967**, *8*, 109.
(6) (a) Donahue, C. J.; Archer, R. D. *J. Am. Chem. Soc.* **1977**, *99*, 6613. (b) Donahue, C. J.; Clark-Motia, D.; Harvey, M. E. *Inorg. Chem.* **1985**, *24*, 801. (c) Donahue, C. J.;Kosinski, E. C.; Martin, V. A. *Inorg. Chem.* **1985**, *24*, 1997.

0020-1669/91/1330-4986$02.50/0

ordinate geometrical isomers can sometimes be separated and that such stereoisomers can be stereochemically rigid. However, in none of these cases[6,7] was it possible to assign a specific structure to any isomer although dodecahedral geometries were believed to be present.

Recently, we have been studying the reactions of the polyhydride complex $ReH_7(PPh_3)_2$ with various organic "acids" (LH) in the hope that these might lead to the release of H_2 and the generation of a reactive, coordinatively unsaturated, rhenium center. By this means we have prepared a series of neutral monohydridorhenium(III) complexes of stoichiometry $ReH(L)_2(PPh_3)_2$, where L represents a chelating monoanionic ligand derived from pyridine-2-carboxylic acid, 1-isoquinolinecarboxylic acid, pyridine-2,3-dicarboxylic acid, 2-hydroxypyridine (hp), 2-hydroxy-6-methylpyridine (mhp), and acetylacetone (acac).[8] These complexes can be oxidized to their corresponding paramagnetic, 17-electron monocationic forms $[ReH(L)_2(PPh_3)_2]^+$,[8,9] which are in some instances quite stable.[10] However, we observed[8] that solutions of $[ReH(mhp)_2(PPh_3)_2]PF_6$ decompose quite readily, and we were also unable to isolate a pure sample of $[ReH(hp)_2(PPh_3)_2]PF_6$. During the course of studies that have been aimed at unraveling the cause of this instability, we have isolated and structurally characterized geometrical isomers of the dihydride complex $[ReH_2(mhp)_2(PPh_3)_2]PF_6$, which are remarkable in that they retain their structural identities in solution. We have also isolated and structurally characterized the seven-coordinate complex $[ReO(mhp)_2(PPh_3)_2]PF_6$, which is the first example of a mononuclear, monooxorhenium(V) complex with a coordination number greater than 6. Details of the synthesis and redox chemistry of the 2-mercaptopyridinato complex $ReH(mp)_2(PPh_3)_2$, which is the sulfur-containing analogue of $ReH(hp)_2(PPh_3)_2$, are also reported. Certain of these results have been described in a preliminary report.[11]

Experimental Section

Starting Materials. The polyhydride complex $ReH_7(PPh_3)_2$ was prepared by the standard literature method.[12] The neutral monohydride complexes $ReH(L)_2(PPh_3)_2$, L = hp or mhp, and the oxidized derivative $[ReH(mhp)_2(PPh_3)_2]PF_6$ were prepared by methods described elsewhere.[8] Cobaltocene was obtained from Strem Chemicals, Inc., while the oxidant $[(\eta^5\text{-}C_5H_5)_2Fe]PF_6$ was prepared as described in the literature.[13] Hexafluorophosphoric acid (60% by weight in water) was obtained from Aldrich Chemical Co., and 1,8-diazabicyclo[5.4.0]-7-undecene (DBU) was obtained from Alfa Products. Other reagents and solvents were obtained from commercial sources. Solvents were thoroughly deoxygenated prior to use.

Reaction Procedures. All reactions were performed under an atmosphere of dry nitrogen.

A. Reaction of $ReH_7(PPh_3)_2$ with 2-Mercaptopyridine. $ReH(mp)_2(PPh_3)_2\cdot 2H_2O$. A mixture of $ReH_7(PPh_3)_2$ (0.200 g, 0.278 mmol) and 2-mercaptopyridine (0.062 g, 0.556 mmol) in 5 mL of acetone was refluxed for 20 min. A large excess of methanol (100 mL) was added to the cooled reaction mixture, which was then stirred for 5 min. The red-orange solid was filtered off, washed with methanol, and dried under vacuum; yield 0.220 g (84%). Anal. Calcd for $C_{46}H_{43}N_2O_2S_2P_2Re$: C, 57.07; H, 4.49. Found, C. 56.95; H, 4.20.

B. Oxidation of $ReH(L)_2(PPh_3)_2$ with $[(\eta^5\text{-}C_5H_5)_2Fe]PF_6$ (L = hp, mp). (i) $[ReH(mp)_2(PPh_3)_2]PF_6\cdot 2H_2O$. A solution of $ReH(mp)_2(PPh_3)_2\cdot 2H_2O$ (0.100 g, 0.103 mmol) and $[(\eta^5\text{-}C_5H_5)_2Fe]PF_6$ (0.040 g, 0.121 mmol) in 5 mL of CH_2Cl_2 was stirred for 10 min. Diethyl ether (50 mL) was added to the solution to precipitate the green product. The precipitate was filtered off and dried under vacuum; yield 0.110 g (95%). Anal. Calcd for $C_{46}H_{43}N_2F_6O_2S_2P_3Re$: C, 50.45; H, 3.78. Found: C, 50.53; H, 3.93.

(ii) $[ReH(hp)_2(PPh_3)_2]PF_6\cdot 2H_2O$. A solution of $ReH(hp)_2(PPh_3)_2\cdot 2H_2O$ (0.050 g, 0.053 mmol) and $[(\eta^5\text{-}C_5H_5)_2Fe]PF_6$ (0.040 g, 0.121 mmol) in 5 mL of CH_2Cl_2 was stirred for 10 min. Diethyl ether (50 mL) was added to the solution to precipitate the purple product. The precipitate was filtered off, washed with water in order to remove unreacted $[(\eta^5\text{-}C_5H_5)_2Fe]PF_6$, and dried under vacuum; yield 0.040 g (69%). Anal. Calcd for $C_{46}H_{43}N_2F_6O_4P_3Re$: C, 51.10; H, 4.02. Found: C, 50.54; H, 3.72.

C. Reduction of $[ReH(L)_2(PPh_3)_2]PF_6$ (L = mp, hp) with $(\eta^5\text{-}C_5H_5)_2Co$. (i) $ReH(mp)_2(PPh_3)_2\cdot 2H_2O$. A solution of $[ReH(mp)_2(PPh_3)_2]PF_6\cdot 2H_2O$ (0.050 g, 0.045 mmol) and $(\eta^5\text{-}C_5H_5)_2Co$ (0.010 g, 0.050 mmol) in 5 mL of acetone was stirred for 10 min. Methanol (50 mL) was added to the solution to precipitate the product; yield 0.030 g (72%).

(ii) $ReH(hp)_2(PPh_3)_2\cdot 2H_2O$. A similar procedure as that described in section C(i) was used to reduce $[ReH(hp)_2(PPh_3)_2]PF_6\cdot 2H_2O$; yield 66%.

D. Protonation Reactions of $ReH(L)_2(PPh_3)_2$ (L = mp, hp, mhp). (i) $[ReH_2(mp)_2(PPh_3)_2]PF_6$. A solution of $ReH(mp)_2(PPh_3)_2\cdot 2H_2O$ (0.100 g, 0.103 mmol) and HPF_6 (0.10 mL, 1.1 mmol) in 5 mL of CH_2Cl_2 was stirred for 5 min. A large excess of diethyl ether (100 mL) was added to the yellow solution. The yellow precipitate was filtered off, washed with diethyl ether, and dried under vacuum; yield 0.095 g (82%).

(ii) $[ReH_2(hp)_2(PPh_3)_2]PF_6\cdot 2H_2O$. A solution of $ReH(hp)_2(PPh_3)_2\cdot 2H_2O$ (0.060 g, 0.064 mmol) and HPF_6 (0.10 mL, 1.1 mmol) in 5 mL of CH_2Cl_2 was stirred for 5 min. Workup as in section D(i) yielded a yellow precipitate, which was filtered off, washed with diethyl ether, and dried under vacuum; yield 0.060 g (86%). Anal. Calcd for $C_{46}H_{44}N_2F_6O_4P_3Re$: C, 51.06; H, 4.11. Found: C, 51.10; H, 4.28.

(iii) *trans*-$[ReH_2(mhp)_2(PPh_3)_2]PF_6\cdot H_2O$. A solution of $ReH(mhp)_2(PPh_3)_2\cdot H_2O$ (0.100 g, 0.106 mmol) and HPF_6 (0.10 mL, 1.1 mmol) in 5 mL of CH_2Cl_2 was stirred for 5 min. Workup as in section D(i) gave a yellow precipitate, which was filtered from the reaction mixture and dried under vacuum; yield 0.095 g (82%). Anal. Calcd for $C_{48}H_{46}N_2F_6O_3P_3Re$: C, 52.79; H, 4.25. Found: C, 52.31; H, 4.17.

E. Formation of *cis*-$[ReH_2(mhp)_2(PPh_3)_2]PF_6$ and $[ReO(L)_2(PPh_3)_2]PF_6$ (L = hp, mhp). (i) *cis*-$[ReH_2(mhp)_2(PPh_3)_2]PF_6$. A solution of $[ReH(mhp)_2(PPh_3)_2]PF_6$ (0.060 g, 0.056 mmol) in CH_2Cl_2 (5 mL) was stirred at room temperature for 3 days. Diethyl ether (50 mL) was added to the resulting yellow solution, and the mixture was then stirred for 5 min to induce precipitation of the product. The yellow precipitate was filtered off and dried under vacuum; yield 0.020 g (33%).

(ii) $[ReO(mhp)_2(PPh_3)_2]PF_6$. In a test tube fitted with a rubber septum, a solution of $[ReH(mhp)_2(PPh_3)_2]PF_6$ (approximately 0.025 g, 0.023 mmol) in 1,2-dichloroethane (3 mL) was layered with heptane (15 mL). The mixture was maintained at ca. 0 °C for approximately 2 weeks. After this period the contents of the tube consisted of a small crop of green crystals and a yellow solution. Green crystals of $[ReO(mhp)_2(PPh_3)_2]PF_6$ were hand-picked from the reaction mixture; yield 0.004 g (16%). The solution was evaporated and the residue dissolved in a minimum of 1,2-dichloroethane before diethyl ether was added to precipitate a quantity of *cis*-$[ReH_2(mhp)_2(PPh_3)_2]PF_6$; yield 0.008 g (30%).

(iii) $[ReO(hp)_2(PPh_3)_2]PF_6$. Green crystals of $[ReO(hp)_2(PPh_3)_2]PF_6$ were obtained using the procedure described in section E(ii), from a dilute solution of $[ReH(hp)_2(PPh_3)_2]PF_6$ in 1,2-dichloroethane; yield 10%. As in section E(ii), a dihydride complex was also formed along with the oxo species. The yield of *cis*-$[ReH_2(hp)_2(PPh_3)_2]PF_6$ obtained under these conditions was approximately 30%.

F. Deprotonation Reactions of $[ReH_2(L)_2(PPh_3)_2]PF_6$ (L = mp, hp, mhp). (i) $ReH(mp)_2(PPh_3)_2$. A solution of $[ReH_2(mp)_2(PPh_3)_2]PF_6$ (0.075 g, 0.070 mmol) in 5 mL of CH_2Cl_2 was treated with NEt_3 (0.10 mL, 0.74 mmol), and the resulting solution was stirred for 10 min. Methanol (50 mL) was added to precipitate the red-orange product, yield 0.52 g (69%). This deprotonation also occurs with the use of DBU in place of NEt_3.

(ii) $ReH(hp)_2(PPh_3)_2$. A solution of $[ReH_2(hp)_2(PPh_3)_2]PF_6$ (0.050 g, 0.048 mmol) in 5 mL of CH_2Cl_2 was treated with DBU (0.1 mL, 0.67 mmol), and the resulting solution was stirred for 10 min. Workup as in section F(i) gave the orange product, yield 0.025 g (58%). This deprotonation does not occur where NEt_3 is used.

(iii) $ReH(mhp)_2(PPh_3)_2$. A procedure similar to that described in section F(i) was used to deprotonate *trans*-$[ReH_2(mhp)_2(PPh_3)_2]PF_6$ (yield 66%), while a procedure like that described in section F(ii) was

(7) Very recently, several eight-coordinate molybdenum(IV) and tungsten(IV) complexes containing *tert*-butyl-substituted 2-hydroxy- and 2-mercaptopyridinato and -pyrimidinato ligands have been prepared. However, only a single isomer of each tetrakis complex was obtained. Donahue, C. J.; Martin, V. A.; Schoenfelner, B. A.; Kosinski, E. C. *Inorg. Chem.* **1991**, *30*, 1588.

(8) Fanwick, P. E.; Leeaphon, M.; Walton, R. A. *Inorg. Chem.* **1990**, *29*, 676.

(9) Leeaphon, M.; Fanwick, P. E.; Walton, R. A. *Inorg. Chem.* **1990**, *29*, 4348.

(10) For example, the rhenium(IV) acac complex $[ReH(acac)_2(PPh_3)_2]PF_6$ is very stable and has been characterized by X-ray crystallography.[8]

(11) Leeaphon, M.; Fanwick, P. E.; Walton, R. A. *J. Am. Chem. Soc.* **1991**, *113*, 1424.

(12) Chatt, J.; Coffey, R. S. *J. Chem. Soc. A* **1969**, 1963.

(13) Hendrickson, D. N.; Sohn, Y. S.; Gray, H. B. *Inorg. Chem.* **1971**, *10*, 1559.

Table I. Crystallographic Data for *trans*-$[ReH_2(mhp)_2(PPh_3)_2]PF_6 \cdot C_2H_4Cl_2$ (**1**), *cis*-$[ReH_2(mhp)_2(PPh_3)_2]PF_6 \cdot (CH_3)_2CO$ (**2**), *cis*-$[ReH_2(mhp)_2(PPh_3)_2]PF_6 \cdot 0.5C_2H_4Cl_2$ (**3**), and $[ReO(mhp)_2(PPh_3)_2]PF_6 \cdot C_2H_4Cl_2$ (**4**)

	1	**2**	**3**	**4**
chem formula	$ReCl_2P_3F_6O_2N_2C_{50}H_{48}$	$ReP_3F_6O_3N_2C_{51}H_{50}$	$ReClP_3F_6O_2N_2C_{49}H_{46}$	$ReCl_2P_3F_6O_3N_2C_{50}H_{46}$
fw	1172.97	1132.09	1123.49	1186.95
space group	$P\bar{1}$ (No. 2)	*Pbca* (No. 61)	$P\bar{1}$ (No. 2)	$P2_1/c$ (No. 14)
a, Å	13.382 (2)	19.292 (2)	15.075 (4)	11.794 (2)
b, Å	13.723 (2)	22.399 (2)	18.640 (4)	14.168 (1)
c, Å	15.593 (2)	22.314 (2)	20.662 (6)	31.359 (5)
α, deg	107.06 (1)	90	114.53 (1)	90
β, deg	96.54 (1)	90	100.44 (2)	110.776 (6)
γ, deg	114.05 (1)	90	98.40 (2)	90
V, Å^3	2408 (2)	9642 (3)	5033 (5)	4899 (2)
Z	2	8	4	4
T, °C	−62	−96	+20	+20
λ(Mo Kα), Å	0.71073	0.71073	0.71073	0.71073
ρ_{calcd}, g cm^{-3}	1.617	1.560	1.482	1.609
μ(Mo Kα), cm^{-1}	28.29	27.17	26.53	27.84
transm coeff	1.00–0.80	1.00–0.80	1.00–0.85	1.00–0.69
R^a	0.023	0.036	0.059	0.041
R^b	0.030	0.049	0.081	0.049

$^a R = \sum||F_o| - |F_c||/\sum|F_o|$. $^b R_w = \{\sum w(|F_o| - |F_c|)^2/\sum w|F_o|^2\}^{1/2}$; $w = 1/\sigma^2(|F_o|)$.

used to deprotonate *cis*-$[ReH_2(mhp)_2(PPh_3)_2]PF_6$ (yield 56%).

G. Formation of $[ReH(mp)_2(PPh_3)_2]PF_6$ from $[ReH_2(mp)_2(PPh_3)_2]PF_6$. A solution of $[ReH_2(mp)_2(PPh_3)_2]PF_6$ (0.035 g, 0.032 mmol) in 3 mL of CH_2Cl_2 was stirred for 12 h. Diethyl ether (20 mL) was added to the resulting green solution to precipitate $[ReH(mp)_2(PPh_3)_2]PF_6$, yield 0.022 g (63%). The orange filtrate was evaporated, and the residue was treated with dichloromethane and methanol to precipitate a small quantity of an orange solid. On the basis of its cyclic voltammetric properties, this orange product was identified as the neutral monohydride complex $ReH(mp)_2(PPh_3)_2$; yield 0.002 g (6%).

Preparation of Single Crystals for Structure Determinations. Crystals of *trans*-$[ReH_2(mhp)_2(PPh_3)_2PF_6$ were grown by the slow diffusion of deoxygenated heptane into a dilute solution of this complex in 1,2-dichloroethane. Crystals of *cis*-$[ReH_2(mhp)_2(PPh_3)_2PF_6$ were grown by the slow diffusion of deoxygenated heptane into dilute solutions of this complex in either acetone (for the low-temperature structure determination) or 1,2-dichloroethane (for the structure determination at room temperature). Crystals of $[ReO(mhp)_2(PPh_3)_2]PF_6$ were obtained directly from the reaction mixture as described in section E(ii).

X-ray Crystallography. The structures of *trans*-$[ReH_2(mhp)_2(PPh_3)_2]PF_6 \cdot C_2H_4Cl_2$ (**1**), *cis*-$[ReH_2(mhp)_2(PPh_3)_2]PF_6 \cdot (CH_3)_2CO$ (**2**, structure determined at −96 °C), *cis*-$[ReH_2(mhp)_2(PPh_3)_2]PF_6 \cdot 0.5C_2H_4Cl_2$ (**3**, structure determined at +20 °C), and $[ReO(mhp)_2(PPh_3)_2]PF_6 \cdot C_2H_4Cl_2$ (**4**) were determined by application of the standard procedures. The basic crystallographic parameters for these complexes are listed in Table I. The cell constants are based on 25 reflections with $21 < \theta < 23°$ for **1** and **2**, $17 < \theta < 22°$ for **3**, and $15 < \theta < 18°$ for **4**. Three standard reflections were measured after 5000 s of beam time during data collection; there were no systematic variations in intensity.

Calculations were performed on a MicroVAX II computer using the Enraf-Nonius structure determination package. Lorentz and polarization corrections were applied to the data. The structures were solved by the use of the Patterson heavy-atom method, which revealed the positions of the Re atoms. The remaining non-hydrogen atoms were located in succeeding difference Fourier syntheses. For **1**, **2**, and **4** the positions for the hydrogen atoms of the PPh_3 and mhp ligands were calculated by assuming idealized geometry and a C–H bond distance of 0.95 Å. We assumed that the value of B(H), i.e., the isotropic equivalent thermal parameter for the hydrogen atoms, was equal to $1.3[B_{eqv}(C)]$ at the time of the inclusion of this parameter in the refinement procedure. While these hydrogen atoms were used in the calculation of F_c, their positions were not refined. The likely positions of the two hydride ligands in the low-temperature structure determinations of **1** and **2** were revealed in difference Fourier maps. They were refined on this assumption to give acceptable Re–H distances (in the range 1.58 (7)–1.64 (4) Å) and positions that accorded with the NMR spectral properties of these complexes (see text).

All four crystals contained lattice solvent molecules. For **1**, a molecule of 1,2-dichloroethane (gauche isomer) was disordered about a general position such that there were two orientations of the pairs of chlorine atoms about a common C–C unit. The four chlorine sites were each refined with a multiplicity of 0.5. This gave a very satisfactory refinement although the thermal parameters of one of these atoms (Cl(4)) were much larger than the others. All non-hydrogen atoms including those of the $C_2H_4Cl_2$ molecule were refined anisotropically. Crystal **2** contained two disordered acetone molecules located about general positions, each of which was refined with half-occupancy. The disorder was such that the acetone oxygen atoms could not be differentiated from the methyl carbon atoms so all were modeled as carbon and refined isotropically (C(1001)–C(1008)). All other non-hydrogen atoms were refined anisotropically. The structure of **3** revealed the presence of one lattice $C_2H_4Cl_2$ molecule (gauche isomer) that was not disordered although the atoms exhibited high thermal motion (carbons refined isotropically, chlorines anisotropically). There are two independent molecules of $[ReH_2(mhp)_2(PPh_3)_2]PF_6$ in the asymmetric unit (space group $P\bar{1}$, $Z = 4$). All non-hydrogen atoms, except the carbon atoms of the triphenylphosphine ligands, were refined anisotropically. Some of the fluorine atoms of the $[PF_6]^-$ anions of **3** showed high thermal motions. The hydride ligands were not located. The crystal of the oxo complex **4** also contained a molecule of lattice $C_2H_4Cl_2$. The fluorine atoms of $[PF_6]^-$ and the atoms of $C_2H_4Cl_2$ had rather large thermal parameters. All non-hydrogen atoms were refined anisotropically.

In all cases an empirical absorption correction was used,[14] the linear absorption coefficients being 28.29 (for **1**), 27.17 (for **2**), 26.53 (for **3**), and 27.84 cm^{-1} (for **4**). No corrections for extinction were applied. The structures were refined by full-matrix least-squares methods where the function minimized was $\sum w(|F_o| - |F_c|)^2$, where w is the weighting factor defined as $w = 1/\sigma^2(F_o)$. Corrections for anomalous scattering were applied to all atoms that were refined anisotropically.[15]

Positional parameters and their errors for all non-hydrogen atoms of **1**–**4**, except the phenyl group atoms and those of any lattice solvent molecules, are listed in Tables II–V. Important intramolecular bond distances and angles for **1**, **2**, and **4** are given in Table VI. The corresponding structural parameters for **3** are available in the supplementary materials. Tables giving full details of the crystal data and data collection parameters (Tables S1–S4), the positional parameters for all atoms (Tables S5–S8), the thermal parameters (Table S9–S12), and complete bond distances (Tables S13–S16) and bond angles (Tables S17–S20) are available as supplementary material.

Physical Measurements. Infrared spectra were recorded as Nujol mulls between KBr plates on a Perkin-Elmer Model 1800 IR Fourier transform (4000–450 cm^{-1}) spectrometer. Electrochemical measurements were carried out by the use of a Bioanalytical Systems Inc. Model CV-1A instrument on dichloromethane solutions that contained 0.1 M tetra-*n*-butylammonium hexafluorophosphate (TBAH) as the supporting electrolyte. $E_{1/2}$ values, determined as $(E_{p,a} + E_{p,c})/2$, were referenced to the silver/silver chloride (Ag/AgCl) electrode at room temperature and are uncorrected for junction potentials. Under our experimental conditions the ferrocenium/ferrocene couple is at $E_{1/2} = +0.47$ V vs Ag/AgCl. ^{1}H NMR spectra were recorded on Varian XL-200 or VXR-500 spectrometers. Resonances were referenced internally to the residual protons in the incompletely deuteriated solvent. $^{31}P\{^1H\}$ NMR spectra were obtained on a Varian XL-200 spectrometer. An internal

(14) Walker, N.; Stuart, D. *Acta Crystallogr., Sect. A Found Crystallogr.* **1983**, *A39*, 158.

(15) (a) Cromer, D. T. *International Tables for X-ray Crystallography*; Kynoch: Birmingham, England, 1974; Vol. IV, Table 2.3.1. (b) For the scattering factors used in the structure solution, see: Cromer, D. T.; Waber, J. T. In ref 15a, Table 2.2B.

Table II. Positional Parameters and Equivalent Isotropic Displacement Parameters (Å²) for the Non-Phenyl Atoms and Nonlattice Solvent Atoms of **1** and Their Estimated Standard Deviations

atom	x	y	z	B,[a] Å²
Re	0.25973 (1)	−0.01770 (1)	0.18057 (1)	1.833 (3)
P(1)	0.16591 (7)	−0.22666 (7)	0.09197 (6)	2.02 (2)
P(2)	0.36388 (7)	0.19491 (7)	0.24115 (6)	2.09 (2)
O(12)	0.1430 (2)	−0.0221 (2)	0.0745 (2)	2.38 (6)
O(22)	0.3677 (2)	−0.0077 (2)	0.0924 (2)	2.62 (6)
N(11)	0.1103 (2)	−0.0164 (2)	0.2081 (2)	2.20 (7)
N(21)	0.4125 (2)	−0.0210 (2)	0.2244 (2)	2.49 (7)
C(12)	0.0669 (3)	−0.0262 (3)	0.1222 (3)	2.45 (8)
C(13)	−0.0413 (3)	−0.0393 (3)	0.0937 (3)	3.4 (1)
C(14)	−0.1006 (3)	−0.0360 (3)	0.1606 (3)	3.9 (1)
C(15)	−0.0549 (3)	−0.0216 (3)	0.2493 (3)	3.8 (1)
C(16)	0.0519 (3)	−0.0126 (3)	0.2739 (3)	2.85 (9)
C(22)	0.4474 (3)	−0.0092 (3)	0.1490 (3)	2.59 (9)
C(23)	0.5504 (3)	−0.0027 (3)	0.1378 (3)	4.1 (1)
C(24)	0.6145 (3)	−0.0104 (4)	0.2080 (4)	4.8 (1)
C(25)	0.5777 (4)	−0.0264 (3)	0.2844 (4)	4.6 (1)
C(26)	0.4738 (3)	−0.0312 (3)	0.2931 (3)	3.4 (1)
H(1)	0.301 (3)	0.045 (3)	0.294 (2)	0.4 (8)*
H(2)	0.229 (3)	−0.086 (3)	0.250 (3)	2 (1)*
P(100)	0.29785 (9)	0.2485 (1)	0.63228 (7)	3.52 (3)
F(101)	0.2696 (2)	0.2618 (2)	0.5360 (2)	4.41 (7)
F(102)	0.2658 (2)	0.3475 (2)	0.6814 (2)	5.71 (8)
F(103)	0.4254 (2)	0.3440 (3)	0.6553 (2)	6.16 (9)
F(104)	0.3315 (2)	0.1533 (2)	0.5826 (2)	5.99 (8)
F(105)	0.1701 (2)	0.1565 (3)	0.6100 (2)	6.44 (9)
F(106)	0.3247 (2)	0.2350 (3)	0.7288 (2)	6.71 (8)

[a] Values for anisotropically refined atoms are given in the form of the isotropic equivalent thermal parameter defined as $(4/3)[a^2\beta(1,1) + b^2\beta(2,2) + c^2\beta(3,3) + ab(\cos\gamma)\beta(1,2) + ac(\cos\beta)\beta(1,3) + bc(\cos\alpha)\beta(2,3)]$. Data for the phenyl group atoms and lattice solvent atoms are available as supplementary material. An asterisk denotes a value for an isotropically refined atom.

Table III. Positional Parameters and Equivalent Isotropic Displacement Parameters (Å²) for the Non-Phenyl Atoms and Nonlattice Solvent Atoms of **2** and Their Estimated Standard Deviations

atom	x	y	z	B,[a] Å²
Re	0.15885 (1)	0.11322 (1)	0.01347 (1)	1.449 (6)
P(1)	0.1741 (1)	0.21983 (9)	0.01246 (9)	1.55 (4)
P(2)	0.2452 (1)	0.03608 (9)	0.0096 (1)	2.07 (4)
P(100)	0.3592 (1)	0.2404 (1)	0.2460 (1)	2.92 (5)
F(101)	0.3423 (6)	0.2684 (6)	0.1879 (4)	17.1 (4)
F(102)	0.4256 (5)	0.2713 (6)	0.2466 (6)	17.7 (5)
F(103)	0.3987 (7)	0.1915 (5)	0.2153 (5)	16.1 (4)
F(104)	0.2908 (6)	0.2065 (5)	0.2475 (7)	17.6 (5)
F(105)	0.3195 (7)	0.2900 (4)	0.2776 (5)	14.8 (4)
F(106)	0.3727 (6)	0.2090 (5)	0.3061 (4)	12.7 (3)
O(3)	0.0980 (3)	0.0357 (2)	0.0041 (2)	2.1 (1)
O(4)	0.0572 (3)	0.1444 (2)	0.0308 (2)	1.9 (1)
N(31)	0.1226 (3)	0.0916 (3)	−0.0742 (3)	1.7 (1)
N(41)	0.1254 (3)	0.1142 (3)	0.1039 (3)	1.9 (1)
C(32)	0.0830 (4)	0.0465 (3)	−0.0523 (4)	2.1 (2)
C(33)	0.0339 (4)	0.0180 (4)	−0.0878 (4)	2.9 (2)
C(34)	0.0291 (5)	0.0355 (4)	−0.1468 (4)	3.6 (2)
C(35)	0.0723 (5)	0.0792 (4)	−0.1695 (4)	3.5 (2)
C(36)	0.1200 (5)	0.1069 (4)	−0.1321 (4)	2.5 (2)
C(37)	0.1705 (5)	0.1524 (4)	−0.1571 (4)	3.1 (2)
C(42)	0.0604 (4)	0.1327 (3)	0.0880 (3)	1.8 (2)
C(43)	0.0069 (5)	0.1374 (4)	0.1294 (4)	2.8 (2)
C(44)	0.0232 (5)	0.1238 (4)	0.1883 (4)	3.7 (2)
C(45)	0.0894 (5)	0.1061 (4)	0.2043 (4)	3.4 (2)
C(46)	0.1412 (5)	0.1030 (4)	0.1615 (4)	2.5 (2)
C(47)	0.2142 (5)	0.0893 (4)	0.1777 (4)	3.5 (2)
H(1)	0.226 (4)	0.136 (3)	0.049 (3)	0 (2)*
H(2)	0.225 (4)	0.134 (4)	−0.023 (4)	1 (2)*

[a] Values for anisotropically refined atoms are given in the form of the isotropic equivalent thermal parameter defined as $(4/3)[a^2\beta(1,1) + b^2\beta(2,2) + c^2\beta(3,3) + ab(\cos\gamma)\beta(1,2) + ac(\cos\beta)\beta(1,3) + bc(\cos\alpha)\beta(2,3)]$. Data for the phenyl group atoms and lattice solvent atoms are available as supplementary material. An asterisk denotes a value for an isotropically refined atom.

Scheme I

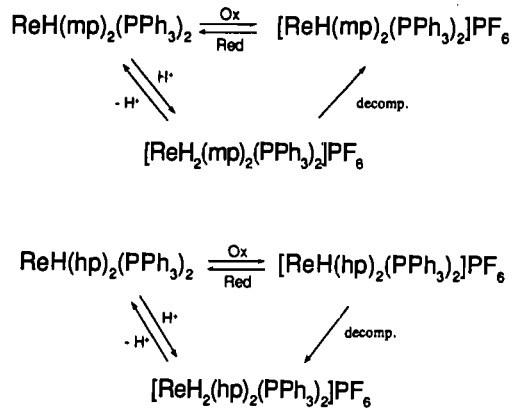

Scheme II

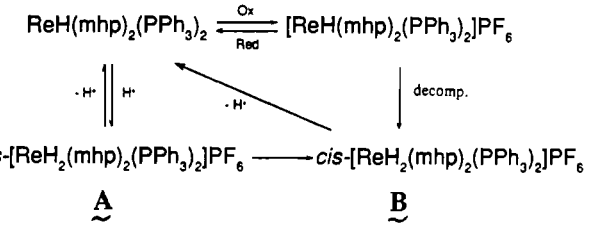

deuterium lock and an external reference, 85% H_3PO_4, were used. Conductivity measurements were performed on acetone solutions of the samples at a concentration of ca. 1.0×10^{-3} M. Measurements were made on an Industrial Instruments Inc. Model RC-16B2 conductivity bridge. EPR spectra of CH_2Cl_2 or acetone/toluene glasses were recorded at ca. −160 °C with a Varian E-109 spectrometer.

Analytical Procedures. Elemental microanalyses were performed by Dr. H. D. Lee of the Purdue University Microanalytical Laboratory.

Results

Most of the chemistry involving the hydrido complexes of Re(III), Re(IV), and Re(V) that is described in this report is summarized in Schemes I and II.

(a) $ReH(L)(PPh_3)_2$ Complexes and Their Oxidized Congeners (L = hp, mhp, mp). As reported earlier,[8] $ReH_7(PPh_3)_2$ reacts with the ligands 2-hydroxypyridine (Hhp) and 2-hydroxy-6-methylpyridine (Hmhp) in acetone to afford the monohydridorhenium(III) complexes $ReH(L)_2(PPh_3)_2$, where L represents the chelating monoanionic ligand derived from Hhp and Hmhp. In the present study we prepared the analogous seven-coordinate complex with the 2-mercaptopyridinate ligand (mp) through the reaction of $ReH_7(PPh_3)_2$ with Hmp in hot toluene. The red-orange crystalline complex, which is of composition $ReH(mp)_2(PPh_3)_2 \cdot 2H_2O$, is soluble in dichloromethane, THF, and acetonitrile but is only slightly soluble in acetone and benzene. Acetone solutions of this complex are essentially nonconducting, with $\Lambda_m \approx 4\ \Omega^{-1}\ cm^2\ mol^{-1}$ for $c_m = 1 \times 10^{-3}$ M. Its IR spectrum (Nujol mull) shows a ν(Re–H) mode at 2070 w cm^{-1} and a broad band at ca. 3400 cm^{-1} due to ν(O–H) of lattice water. The ^1H NMR spectrum of $ReH(mp)_2(PPh_3)_2$ (measured in C_6D_6)[16] consists of a fairly complex set of phenyl and pyridyl resonances at $\approx\delta$ +7.2, and a binomial triplet at δ −1.9 that is assignable to the Re–*H* resonance. The chemical shift for Re–*H*, as well as the P–H coupling constant of 63 Hz, is characteristic of other seven-coordinate monohydridorhenium(III) complexes.[8,17] Integration is in accord with

(16) When the ^1H NMR spectrum of $ReH(mp)_2(PPh_3)_2$ is recorded in CD_2Cl_2, the phenyl proton resonances appear as a multiplet at $\approx\delta$ +7.2, while three of the four pyridyl resonances are distinguishable as two triplets at δ +6.83 and δ +6.06, and a doublet centered at δ + 6.30 ($J \approx 8$ Hz). It is assumed that another doublet pyridyl resonance is obscured by phenyl resonances. The hydride resonance however, is not well-resolved in this solvent. It appears as a broad resonance at $\delta \approx -2.9$.

(17) Allison, J. D.; Moehring, G. A.; Walton, R. A. *J. Chem. Soc., Dalton Trans.* **1986**, 67.

Table IV. Positional Parameters and Equivalent Isotropic Displacement Parameters (Å²) for the Non-Phenyl Atoms and Nonlattice Solvent Atoms of **3** and Their Estimated Standard Deviations

atom	*x*	*y*	*z*	*B*,[a] Å²
Re(1)	0.22914 (4)	0.69655 (4)	0.54670 (3)	2.84 (1)
Re(2)	0.05416 (4)	−0.18724 (3)	0.03123 (3)	2.69 (1)
P(11)	0.3147 (3)	0.8279 (2)	0.6466 (2)	3.2 (1)
P(12)	0.2314 (3)	0.6420 (2)	0.4192 (2)	3.1 (1)
P(21)	0.0397 (3)	−0.2385 (2)	0.1196 (2)	3.1 (1)
P(22)	0.1332 (3)	−0.2224 (2)	−0.0655 (2)	3.0 (1)
O(11)	0.2033 (7)	0.6854 (6)	0.6392 (5)	3.5 (3)
O(12)	0.1245 (7)	0.5871 (6)	0.4983 (6)	3.8 (3)
O(21)	0.0459 (7)	−0.0963 (5)	−0.0032 (5)	3.3 (3)
O(22)	−0.0425 (7)	−0.1302 (6)	0.0836 (5)	3.6 (3)
N(111)	0.3119 (8)	0.6352 (7)	0.5904 (6)	3.2 (3)
N(121)	0.0879 (8)	0.7025 (7)	0.5203 (6)	3.3 (3)
N(211)	0.1543 (8)	−0.0726 (7)	0.0949 (6)	3.0 (3)
N(221)	−0.0901 (8)	−0.2385 (7)	−0.0263 (6)	3.1 (3)
C(112)	0.260 (1)	0.6383 (9)	0.6375 (8)	3.7 (4)
C(113)	0.269 (1)	0.595 (1)	0.6803 (9)	5.5 (5)
C(114)	0.337 (1)	0.552 (1)	0.673 (1)	5.9 (5)
C(115)	0.394 (1)	0.551 (1)	0.623 (1)	5.7 (6)
C(116)	0.380 (1)	0.5938 (9)	0.5827 (9)	3.9 (4)
C(117)	0.441 (1)	0.600 (1)	0.5342 (9)	4.5 (5)
C(122)	0.056 (1)	0.6243 (9)	0.5007 (8)	3.5 (4)
C(123)	−0.038 (1)	0.585 (1)	0.4843 (9)	4.7 (5)
C(124)	−0.100 (1)	0.635 (1)	0.489 (1)	5.7 (6)
C(125)	−0.067 (1)	0.717 (1)	0.508 (1)	6.0 (6)
C(126)	0.031 (1)	0.752 (1)	0.5232 (9)	5.0 (5)
C(127)	0.070 (1)	0.840 (1)	0.537 (1)	5.8 (6)
C(212)	0.112 (1)	−0.0393 (9)	0.0545 (8)	3.3 (4)
C(213)	0.137 (1)	0.0425 (9)	0.0727 (9)	4.4 (5)
C(214)	0.211 (1)	0.090 (1)	0.1337 (9)	5.0 (5)
C(215)	0.258 (1)	0.054 (1)	0.1742 (9)	4.8 (5)
C(216)	0.228 (1)	−0.026 (1)	0.1542 (8)	3.9 (5)
C(217)	0.281 (1)	−0.068 (1)	0.1930 (9)	4.8 (5)
C(222)	−0.115 (1)	−0.1786 (9)	0.0276 (8)	3.5 (4)
C(223)	−0.207 (1)	−0.171 (1)	0.0213 (9)	5.3 (5)
C(224)	−0.274 (1)	−0.232 (1)	−0.0428 (9)	5.7 (5)
C(225)	−0.247 (1)	−0.296 (1)	−0.0986 (9)	5.2 (5)
C(226)	−0.154 (1)	−0.2971 (9)	−0.0871 (8)	3.6 (4)
C(227)	−0.122 (1)	−0.366 (1)	−0.1422 (9)	4.7 (5)
P(1000)	0.3019 (4)	0.2047 (3)	0.4093 (3)	5.7 (2)
P(2000)	0.5323 (5)	0.4905 (4)	0.8526 (4)	8.0 (2)
F(11)	0.306 (1)	0.1187 (7)	0.3506 (7)	8.9 (4)
F(12)	0.269 (2)	0.1658 (9)	0.4546 (7)	16.4 (6)
F(13)	0.406 (1)	0.224 (1)	0.450 (1)	14.3 (8)
F(14)	0.296 (1)	0.2907 (8)	0.4653 (8)	11.6 (6)
F(15)	0.334 (1)	0.2415 (8)	0.3586 (7)	12.1 (5)
F(16)	0.202 (1)	0.189 (1)	0.362 (1)	13.6 (7)
F(21)	0.532 (2)	0.425 (2)	0.784 (2)	30 (1)
F(22)	0.437 (1)	0.457 (2)	0.852 (1)	21 (1)
F(23)	0.496 (2)	0.534 (1)	0.813 (1)	26.4 (8)
F(24)	0.537 (2)	0.564 (1)	0.921 (1)	22 (1)
F(25)	0.634 (1)	0.525 (1)	0.853 (1)	15.1 (7)
F(26)	0.578 (1)	0.461 (1)	0.905 (1)	20.7 (8)

[a] Values for anisotropically refined atoms are given in the form of the isotropic equivalent thermal parameter defined as $(4/3)[a^2\beta(1,1) + b^2\beta(2,2) + c^2\beta(3,3) + ab(\cos\gamma)\beta(1,2) + ac(\cos\beta)\beta(1,3) + bc(\cos\alpha)\beta(2,3)]$. Data for the phenyl group atoms and lattice solvent atoms are available as supplementary material.

the proposed stoichiometry of the complex. A singlet at δ +26.6 is observed in the $^{31}P\{^1H\}$ NMR spectrum of the complex and a doublet (J_{P-H} = 64 Hz) in the ^{31}P NMR spectrum, confirming the presence of a single hydrido ligand.

The electrochemical properties of this complex are similar to those of other, related monohydride complexes.[8] Cyclic voltammetric measurements on solutions of this complex in 0.1 M TBAH in CH_2Cl_2 show a reversible couple at $E_{1/2}$ = −0.14 V vs Ag/AgCl that corresponds to a one-electron oxidation of the complex and an irreversible oxidation at $E_{p,a}$ = +0.93 V. The latter process has product waves associated with it at $E_{p,a}$ = +1.05 and +1.27 V. This complex has been electrochemically oxidized (+0.40 V) to generate solutions that contain the green monocation; this species can be reduced back to the neutral precursor, upon bulk

Table V. Positional Parameters and Equivalent Isotropic Displacement Parameters (Å²) for the Non-Phenyl Atoms and Nonlattice Solvent Atoms of **4** and Their Estimated Standard Deviations

atom	*x*	*y*	*z*	*B*,[a] Å²
Re	0.03586 (3)	0.06671 (3)	0.34771 (1)	2.589 (6)
P(1)	−0.1904 (2)	0.0600 (2)	0.32496 (8)	3.15 (5)
P(2)	0.2548 (2)	0.1015 (2)	0.36224 (8)	3.01 (5)
O(1)	0.0612 (5)	−0.0378 (4)	0.3757 (2)	3.5 (1)
O(10)	0.0120 (5)	0.1359 (4)	0.2853 (2)	2.7 (1)
O(20)	0.0054 (5)	0.2136 (4)	0.3529 (2)	3.5 (1)
N(11)	0.0178 (6)	−0.0160 (5)	0.2868 (2)	2.8 (2)
N(21)	0.0598 (6)	0.1295 (6)	0.4141 (2)	3.9 (2)
C(12)	0.0099 (8)	0.0606 (6)	0.2605 (3)	3.3 (2)
C(13)	−0.0028 (8)	0.0547 (7)	0.2149 (3)	3.9 (2)
C(14)	0.0006 (9)	−0.0337 (8)	0.1983 (3)	4.8 (3)
C(15)	0.0093 (9)	−0.1137 (7)	0.2253 (3)	4.5 (2)
C(16)	0.0180 (8)	−0.1049 (7)	0.2699 (3)	4.0 (2)
C(17)	0.029 (1)	−0.1854 (8)	0.3011 (4)	6.1 (3)
C(22)	0.0310 (8)	0.2167 (7)	0.3968 (3)	4.3 (2)
C(23)	0.026 (1)	0.2932 (9)	0.4238 (3)	6.3 (3)
C(24)	0.055 (1)	0.273 (1)	0.4699 (4)	8.1 (4)
C(25)	0.086 (1)	0.186 (1)	0.4872 (3)	7.5 (4)
C(26)	0.0901 (9)	0.110 (1)	0.4593 (3)	6.0 (3)
P(100)	0.1424 (3)	0.6610 (2)	0.4338 (1)	5.42 (8)
F(101)	0.077 (1)	0.647 (1)	0.4635 (3)	22.6 (5)
F(102)	0.027 (1)	0.665 (1)	0.3951 (5)	21.6 (6)
F(103)	0.153 (1)	0.7645 (8)	0.4393 (6)	20.3 (7)
F(104)	0.258 (1)	0.652 (1)	0.4686 (5)	25.6 (6)
F(105)	0.134 (2)	0.5558 (8)	0.4269 (6)	20.7 (6)
F(106)	0.202 (1)	0.680 (2)	0.4007 (4)	23.5 (7)

[a] Values for anisotropically refined atoms are given in the form of the isotropic equivalent thermal parameter defined as $(4/3)[a^2\beta(1,1) + b^2\beta(2,2) + c^2\beta(3,3) + ab(\cos\gamma)\beta(1,2) + ac(\cos\beta)\beta(1,3) + bc(\cos\alpha)\beta(2,3)]$. Data for the phenyl group atoms and lattice solvent atoms are available as supplementary material.

electrolysis at ca. −0.40 V. The oxidation at −0.14 V can also be accessed with the use of the one-electron oxidant $[(\eta^5\text{-}C_5H_5)_2Fe]PF_6$ in dichloromethane. The resulting complex $[ReH(mp)_2(PPh_3)_2]PF_6$ has electrochemical properties very similar to those of the neutral precursor, except that the process at $E_{1/2}$ = −0.14 V now corresponds to a reduction. This suggests that little structural rearrangement has occurred as a result of the electron transfer. While the IR spectrum shows an intense band at 840 cm⁻¹ due to ν(P-F) of $[PF_6]^-$, the ν(Re–H) bands are too weak to be detected. Conductivity measurements on acetone solutions of $[ReH(mp)_2(PPh_3)_2]PF_6$ show that it is a 1:1 electrolyte with Λ_m = 118 Ω^{-1} cm² mol⁻¹ for $c_m = 1 \times 10^{-3}$ M. Dichloromethane solutions of $[ReH(mp)_2(PPh_3)_2]PF_6$ are ESR-active at low temperatures (−160 °C). The X-band spectrum shows a broad feature at $g \approx 1.9$ (showing Re hyperfine) and an additional feature at $g \approx 2.7$. The paramagnetism of this complex was confirmed by a magnetic moment determination on a dichloromethane solution by use of the Evans method (μ_{eff} = 1.6 (±0.1) μ_B).[18] Rereduction to the neutral precursor can be accomplished through the use of $(\eta^5\text{-}C_5H_5)_2Co$ in acetone.

This 17-electron monohydrido cation[19] is appreciably more stable than its mhp analogue $[ReH(mhp)_2(PPh_3)_2]PF_6$, which was reported previously.[8] However, we had been unsuccessful in our previous attempts[8] to prepare a pure sample of the oxidized hp complex $[ReH(hp)_2(PPh_3)_2]PF_6$. When 1 equiv of $[(\eta^5\text{-}C_5H_5)_2Fe]PF_6$ is used as the oxidant in dichloromethane the solution acquires a purple color, which is associated with the formation of the oxidized species $[ReH(hp)_2(PPh_3)_2]PF_6$. However, rapid decomposition occurred[8] before $[ReH(hp)_2(PPh_3)_2]PF_6$ could be precipitated from solution. We now find that when more than 1 equiv of oxidant is used, the cation can be isolated along

(18) Evans, D. F. *J. Chem. Soc.* **1959**, 2003.

(19) Electronic absorption spectral data (recorded in CH_2Cl_2) for this complex and its neutral precursor are as follows (λ_{max} values in nm are quoted and molar extinction coefficients are given in parentheses): $ReH(mp)_2(PPh_3)_2$, 412 (8400), 510 sh; $[ReH(mp)_2(PPh_3)_2]PF_6$, 383 (6400), 564 (1400), 671 (2000).

Table VI. Comparison of Important Bond Distances (Å) and Bond Angles (deg) for **1**, **2** and **4**[a]

1		2		4	
		Bond Distances			
Re–H(1)	1.64 (4)	Re–H(1)	1.61 (6)	Re–O(1)	1.692 (5)
Re–H(2)	1.61 (4)	Re–H(2)	1.58 (7)		
Re–P(1)	2.461 (1)	Re–P(1)	2.406 (2)	Re–P(1)	2.507 (2)
Re–P(2)	2.473 (1)	Re–P(2)	2.402 (2)	Re–P(2)	2.507 (2)
Re–N(11)	2.098 (3)	Re–N(31)	2.133 (5)	Re–N(11)	2.185 (7)
Re–N(21)	2.103 (3)	Re–N(41)	2.120 (5)	Re–N(21)	2.188 (7)
Re–O(12)	2.111 (3)	Re–O(3)	2.106 (4)	Re–O(10)	2.118 (5)
Re–O(22)	2.097 (3)	Re–O(4)	2.118 (4)	Re–O(20)	2.128 (6)
		Bond Angles			
P(1)–Re–P(2)	168.76 (3)	P(1)–Re–P(2)	128.97 (6)	P(1)–Re–P(2)	169.34 (8)
P(1)–Re–O(12)	82.63 (7)	P(1)–Re–O(4)	77.7 (1)	P(1)–Re–O(20)	82.4 (2)
P(1)–Re–N(11)	93.85 (9)	P(1)–Re–N(41)	92.0 (2)	P(1)–Re–N(21)	93.0 (2)
O(12)–Re–N(11)	61.8 (1)	O(4)–Re–N(41)	62.6 92)	O(20)–Re–N(21)	59.8 (3)
O(22)–Re–N(21)	61.8 (1)	O(3)–Re–N(31)	62.6 (2)	O(10)–Re–N(11)	60.0 (2)
N(11)–Re–N(21)	149.1 (1)	N(31)–Re–N(41)	140.9 (2)	N(11)–Re–N(21)	171.5 (3)
O(12)–Re–O(22)	87.4 (1)	O(3)–Re–O(4)	76.9 (2)	O(10)–Re–O(20)	69.4 (2)
H(1)–Re–H(2)	56 (2)	H(1)–Re–H(2)	61 (3)	O(1)–Re–H(11)	85.8 (3)
P(1)–Re–H(2)	70 (2)	P(1)–Re–H(2)	67 (2)	O(1)–Re–N(11)	85.8 (3)
P(2)–Re–H(1)	65 (1)	P(2)–Re–H(1)	72 (2)	P(1)–Re–O(1)	95.1 (2)

[a] Numbers in parameters are estimated standard deviations in the least significant digits.

with excess oxidant, which can be easily washed from the isolated solid with water. The complex $[ReH(hp)_2(PPh_3)_2]PF_6 \cdot 2H_2O$ has many of the same properties as its mp analogue. While the mp complex is green, $[ReH(hp)_2(PPh_3)_2]PF_6$ is a purple solid which is soluble in a variety of solvents such as dichloromethane, THF, acetone and acetonitrile. Conductivity measurements on solutions of $[ReH(hp)_2(PPh_3)_2]PF_6$ in acetone ($c_m = 1 \times 10^{-3}$ M) confirm it to be a 1:1 electrolyte ($\Lambda_m \approx 110\ \Omega^{-1}\ cm^2\ mol^{-1}$). The IR spectrum of this complex (Nujol mull) shows a ν(Re–H) mode at 2016 w cm^{-1} and ν(P–F) of the PF_6^- anion at 840 cm^{-1}. This complex is expected to be paramagnetic, and consistent with this we find $\mu_{eff} = 1.7\ (\pm 0.1)\ \mu_B$ for a dichloromethane solution (as determined by the Evans method).[18] Dichloromethane solutions of this complex also display an X-band ESR spectrum at low temperature (−160 °C) which consists of two broad features spanning the range 1.7–5.2 kG, at $g \approx 1.7$ (with Re hyperfine) and $g \approx 3.1$.

The electrochemistry of this complex is similar to that of the neutral precursor $ReH(hp)_2(PPh_3)_2$ ($E_{1/2}(ox) = +0.02$ V and $E_{p,a} = 1.10$ V in 0.1 M TBAH in CH_2Cl_2)[8] except that the reversible process now corresponds to a reduction. The similarities in the cyclic voltammograms of the neutral and the oxidized species imply that very little structural rearrangement has occurred in the redox process. The subsequent reduction of the monocation is possible with the use of the one-electron reductant $(\eta^5\text{-}C_5H_5)_2Co$ in acetone.

(b) Decomposition of the 17-Electron Complexes $[ReH(L)_2(PPh_3)_2]PF_6$ in Solution and Formation of the Dihydrides $[ReH_2(L)_2(PPh_3)_2]PF_6$. The stabilities of the complexes $[ReH(L)_2(PPh_3)_2]PF_6$ vary considerably depending upon the nature of L. The mp complex is by far the most stable, with solutions in a variety of solvents showing little sign of decomposition even after several weeks. On the other hand, the much more rapid decompositions of the hp and mhp complexes lead to some unexpected and novel results. The oxidized complex $[ReH(hp)_2(PPh_3)_2]PF_6$ is stable as a solid for several days in an inert atmosphere although its eventual decomposition leads to an unidentifiable product. Solutions of the hp-containing complex in deoxygenated solvents such as dichloromethane, 1,2-dichloroethane, acetone, THF, acetonitrile, nitrobenzene, methanol, and ethanol were found to decompose quite rapidly as reflected by a color change from purple to pale yellow. The product which is precipitated from this solution (upon addition of diethyl ether) is a yellow solid which has been characterized as the dihydride complex $[ReH_2(hp)_2(PPh_3)_2]PF_6$. Because this product appears to form regardless of the solvent that is used and because yields of this product are relatively low (ca. 30%), it is assumed that this dihydride complex is produced from a disproportionation reaction of the monohydride complex $[ReH(hp)_2(PPh_3)_2]PF_6$, although no direct evidence of this has been obtained. However, the electronic absorption spectrum of a solution of $[ReH(hp)_2(PPh_3)_2]PF_6$ in CH_2Cl_2 ($\lambda_{max} = 540$ ($\epsilon = 1300$)) can be monitored; its conversion to $[ReH_2(hp)_2(PPh_3)_2]PF_6$ ($\lambda_{max} = 430$ sh and 390 ($\epsilon = 2300$)) is clean with an isosbestic point at 460 nm. The yield of dihydride is not increased by exposing the solutions to air or upon the addition of small amounts of water to these solutions, and we have not been successful in identifying the fate of the major portion of the rhenium. However, addition of heptane to the dichloromethane and 1,2-dichloroethane solutions of $[ReH(hp)_2(PPh_3)_2]PF_6$ produce yellow $[ReH_2(hp)_2(PPh_3)_2]PF_6$, which is admixed with small quantities of green crystalline $[ReO(hp)_2(PPh_3)_2]PF_6$ (ca. 10%) that can be separated by hand. The latter complex was identified by IR spectroscopy (Nujol mull; ν(Re=O) at 943 m cm^{-1} and ν(P–F) at 838 s cm^{-1}).

Since $[ReH_2(hp)_2(PPh_3)_2]PF_6$ is formally the product of protonating $ReH(hp)_2(PPh_3)_2$ with HPF_6, we investigated this as a route to the production of this dihydride and found that it is formed in very high yield (ca. 90%) by such a procedure. Similarly, the protonation of $ReH(mp)_2(PPh_3)_2$ with HPF_6 in dichloromethane affords $[ReH_2(mp)_2(PPh_3)_2]PF_6$. However, while $[ReH_2(hp)_2(PPh_3)_2]PF_6$ is very stable both in the solid state and in solution, the related mp complex decomposes to the monohydrido cationic species $[ReH(mp)_2(PPh_3)_2]PF_6$ in dichloromethane, along with a small quantity of $ReH(mp)_2(PPh_3)_2$. This process involves H_2 loss (as monitored by ^1H NMR spectroscopy). Both $[ReH_2(hp)_2(PPh_3)_2]PF_6$ and $[ReH_2(mp)_2(PPh_3)_2]PF_6$ are easily deprotonated to reform the neutral monohydrides although the hp complex requires a stronger base (DBU) for the deprotonation to occur. This implies that of the two complexes $ReH(mp)_2(PPh_3)_2$ and $ReH(hp)_2(PPh_3)_2$ the latter one is the more basic of the pair since its conjugate acid $[ReH_2(hp)_2(PPh_3)_2]^+$ is more difficult to deprotonate than $[ReH_2(mp)_2(PPh_3)_2]^+$. The ease of decomposition of $[ReH_2(mp)_2(PPh_3)_2]^+$ to $[ReH(mp)_2(PPh_3)_2]^+$, via H_2 loss, illustrates the increased stability of $[ReH(mp)_2(PPh_3)_2]^+$ over that of $[ReH(hp)_2(PPh_3)_2]^+$.

Some of the more important properties of $[ReH_2(mp)_2(PPh_3)_2]PF_6$ and $[ReH_2(hp)_2(PPh_3)_2]PF_6$ are summarized in Table VII. In addition, solutions of these two complexes in acetone (ca. 1×10^{-3} M) have conductivities typical of 1:1 electrolytes ($\Lambda_m = 111$–$113\ \Omega^{-1}\ cm^2\ mol^{-1}$). The ^1H NMR spectra of both contain phenyl and pyridyl resonances around δ +7.2 and a triplet ($J_{P-H} \approx 48$ Hz) assignable to the Re–*H* resonance (Table VII). The slight downfield shift and decrease in the P–H coupling constant for these complexes compared to the parent neutral monohydrides is commonly observed for protonated rhenium hydride complexes.[20] The integration of these spectra accord with

Table VII. Properties of the Dihydrido Complexes $[ReH_2(L)_2(PPh_3)_2]PF_6$

complex	IR data,[a] cm^{-1}		^1H NMR data,[b] δ		$^{31}P\{^1H\}$NMR data,[b] δ	CV potentials,[c] V	
	ν(Re–H)	ν(P–F)	Re–*H*	C*H*$_3$(mhp)		$E_{p,a}$	$E_{p,c}$
$[ReH_2(mp)_2(PPh_3)_2]PF_6$	2032 w	840 s	+0.44 (t, J_{P-H} = 49 Hz)		+20.2 (s)	+1.0	−1.36
$[ReH_2(hp)_2(PPh_3)_2]PF_6 \cdot 2H_2O$	2100 w, 2092 w	840 s	+4.19 (t, J_{P-H} = 47 Hz)		+30.2 (s)	+1.5	−1.47
cis-$[ReH_2(mhp)_2(PPh_3)_2]PF_6$	2080 w	842 s	+4.65 (t, J_{P-H} = 46 Hz)	+1.30 (s)	+25.9 (s)	+1.59	−1.54
trans-$[ReH_2(mhp)_2(PPh_3)_2]PF_6 \cdot H_2O$	2070 w, 2046 vw	840 s	+6.66 (dd)[d]	+1.90 (s)	+14.3 (s)	+1.51	−1.48

[a] Recorded as Nujol mulls. Abbreviations: w = weak; s = strong. [b] Recorded in CD_2Cl_2. Abbreviations: t = triplet; s = singlet; dd = doublet of doublets. The resonances due to the $[PF_6]^-$ anions are present as septets centered at ca. δ −144. [c] Measured in 0.1 M TBAH in CH_2Cl_2 solutions and referenced to the Ag/AgCl electrode with a scan rate of 200 mV s^{-1} at a Pt-bead electrode. [d] For a discussion of this pattern and the associated coupling constants see the Results section of text.

the formulations of these two complexes. Their $^{31}P\{^1H\}$ NMR spectra are singlets, while in each case the ^{31}P spectrum consists of a triplet (with J_{P-H} = 45–50 Hz) thus confirming the presence of two hydride ligands.

The 17-electron, paramagnetic monohydrido mhp complex $[ReH(mhp)_2(PPh_3)_2]PF_6$ resembles its hp analogue (vide supra) in being stable in the solid state for several weeks. Its solutions decompose to produce $[ReH_2(mhp)_2(PPh_3)_2]PF_6$ as the major product.[21] For reasons that will become apparent, this product will be labeled as *cis*-$[ReH_2(mhp)_2(PPh_3)_2]PF_6$. The yields are low (for example, ca. 33% in dichloromethane), and the reaction course is not affected in any major way by the choice of solvent, the addition of small amounts of water, or exposure of the solutions to air or oxygen. However, the rate of conversion to the dihydride is enhanced by warming the solutions. When solutions of $[ReH(mhp)_2(PPh_3)_2]PF_6$ in 1,2-dichloroethane are layered with heptane and set aside for 2 weeks, a separable mixture of crystalline *cis*-$[ReH_2(mhp)_2(PPh_3)_2]PF_6$ (yellow crystals) and $[ReO(mhp)_2(PPh_3)_2]PF_6$ (green crystals) is formed. This reaction therefore resembles the behavior of $[ReH(hp)_2(PPh_3)_2]PF_6$ under similar conditions (vide supra). The identity of the oxorhenium complex was confirmed by an X-ray structure analysis of a single crystal of composition $[ReO(mhp)_2(PPh_3)_2]PF_6 \cdot C_2H_4Cl_2$ (**4**). These data are presented in Tables I, V, and VI, and an ORTEP representation of the structure of the seven-coordinate $[ReO(mhp)_2(PPh_3)_2]^+$ cation is given in Figure 1. The Nujol mull IR spectrum of this complex shows a ν(Re=O) mode at 966 m cm^{-1}, while the cyclic voltammogram of a solution in 0.1 M TBAH in CH_2Cl_2 reveals an irreversible reduction at $E_{p,c}$ = −0.83 V vs Ag/AgCl. Its ^{31}P NMR spectrum (recorded in CD_2Cl_2) shows a singlet at δ +9.6, and its ^1H NMR spectrum shows expected peaks due to the PPh_3 and mhp ligands; the methyl resonance of mhp is at δ +2.29.

This dihydrido complex is soluble in polar solvents such as dichloromethane, acetone, acetonitrile and THF. Its spectroscopic and electrochemical properties, which are summarized in Table VII, resemble closely those of $[ReH_2(hp)_2(PPh_3)_2]PF_6$. Like the hp complex, *cis*-$[ReH_2(mhp)_2(PPh_3)_2]PF_6$ behaves as a 1:1 electrolyte in acetone (Λ_m = 114 Ω^{-1} cm^2 mol^{-1} for $c_m = 1 \times 10^{-3}$ M). Their ^1H and $^{31}P\{^1H\}$ NMR spectra closely resemble one another (Table VII). The ^1H NMR spectrum of *cis*-$[ReH_2(mhp)_2(PPh_3)_2]PF_6$ is shown in Figure S2. Its ^{31}P NMR spectrum consists of a triplet (J_{P-H} = 49 Hz); this confirms the presence of two hydride ligands.

To resolve any structural questions, an X-ray crystal structure determination was carried out at +20 °C on a crystal of *cis*-$[ReH_2(mhp)_2(PPh_3)_2]PF_6 \cdot 0.5C_2H_4Cl_2$ (**3**). There are two crystallographically independent molecules in the unit cell, and one molecule of 1,2-dichloroethane (gauche isomer) in the asymmetric unit. While the structure refined satisfactorily and revealed clearly that part of the coordination geometry that consisted of two chelating mhp ligands and the two PPh_3 ligands, the hydride ligands were not located. The crystal data and data collection parameters for **3** are given in Table I while the positional parameters for key atoms are listed in Table IV. An ORTEP representation of the structure of **3** is available in the supplementary material (Figure S1) along with a compilation of the important bond distances and bond angles (Tables S11 and S15).

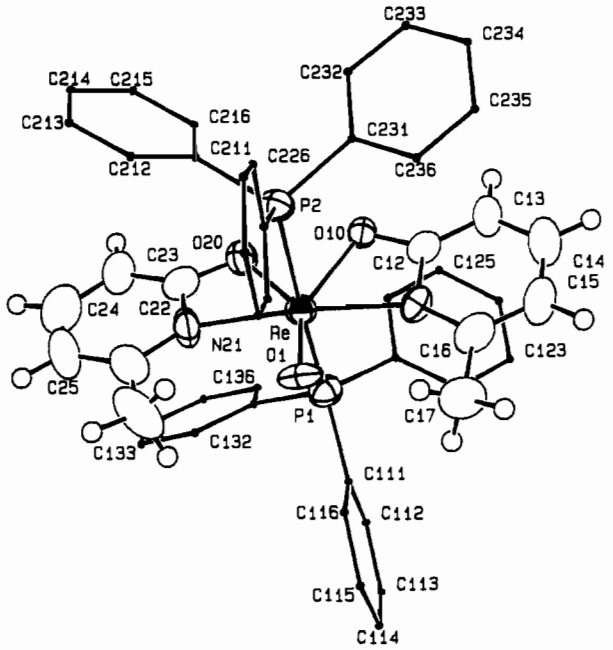

Figure 1. ORTEP representation of the rhenium-containing cation of **4** showing the atomic numbering scheme. The thermal ellipsoids are drawn at the 50% probability level.

In order to obtain a more satisfactory structure, we decided to attempt to obtain crystals of *cis*-$[ReH_2(mhp)_2(PPh_3)_2]PF_6$ in which there was only one independent molecule in the unit cell and to collect data at low temperature. Crystals of composition *cis*-$[ReH_2(mhp)_2(PPh_3)_2]PF_6 \cdot (CH_3)_2CO$ (**2**) proved to be satisfactory, and the subsequent structure determination (see Tables I, III, and VI) showed a structure essentially identical to that of **3**, except for the location and refinement of the two hydride ligands in the crystal of **2** (see Figure 2).

Since the protonation of $ReH(hp)_2(PPh_3)_2$ by HPF_6 gives a complex $[ReH_2(hp)_2(PPh_3)_2]PF_6$, which is identical with that obtained by decomposition of solutions of $[ReH(hp)_2(PPh_3)_2]PF_6$, we next investigated the reaction of $ReH(mhp)_2(PPh_3)_2$ with HPF_6 with the expectation that this would provide a more convenient route to *cis*-$[ReH_2(mhp)_2(PPh_3)_2]PF_6$. To our surprise, although this reaction proceeds in the expected fashion to give a compound of composition $[ReH_2(mhp)_2(PPh_3)_2]PF_6$ in essentially quantitative yield, its properties are distinctly different from those of *cis*-$[ReH_2(mhp)_2(PPh_3)_2]PF_6$. This yellow-orange product, which

(20) Some recent examples are as follows: (a) Luo, X.; Crabtree, R. H. *J. Am. Chem. Soc.* **1990**, *112*, 6912. (b) Heinekey, D. M.; Millar, J. M.; Koetzle, T. F.; Payne, N. G.; Zilm, K. W. *J. Am. Chem. Soc.* **1990**, *112*, 909. (c) Costello, M. T.; Fanwick, P. E.; Meyer, K. E.; Walton, R. A. *Inorg. Chem.* **1990**, *29*, 4437.

(21) Electronic absorption spectral data (recorded in CH_2Cl_2) for the mhp derivatives are as follows: (λ_{max} values in nm are quoted and molar extinction coefficients are given in parentheses): $[ReH(mhp)_2(PPh_3)_2]PF_6$, 570 (1200); *cis*-$[ReH_2(mhp)_2(PPh_3)_2]PF_6$, 370 (≈2000), 420 sh; *trans*-$[ReH_2(mhp)_2(PPh_3)_2]PF_6$, ≈430 sh. In the conversion of the monohydride cation to the cis dihydride complex, an isosbestic point is observed at 455 nm.

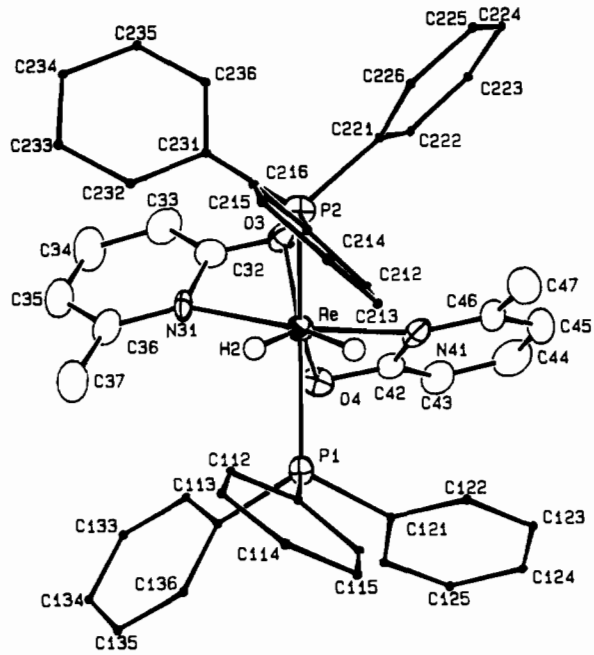

Figure 2. ORTEP representation of the rhenium-containing cation of **2** showing the atomic numbering scheme. The thermal ellipsoids are drawn at the 50% probability level.

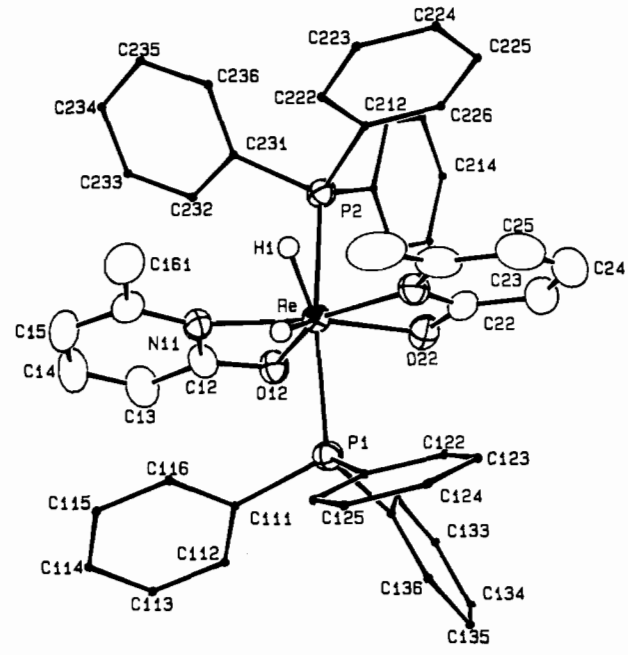

Figure 3. ORTEP representation of the rhenium-containing cation of **1** showing the atomic numbering scheme. The thermal ellipsoids are drawn at the 50% probability level.

is a different isomeric form, is designated *trans*-$[ReH_2(mhp)_2(PPh_3)_2]PF_6$. It has solubility properties similar to those of the cis isomer and likewise behaves as a 1:1 electrolyte (Λ_m = 121 Ω^{-1} cm^2 mol^{-1} for $c_m = 1 \times 10^{-3}$ M). Its other properties are presented in Table VII. The ^{1}H NMR spectrum (recorded at 200 and 500 MHz) has a hydride resonance at δ +6.66 that has the appearance of a doublet of doublets (see Figure S2) implying that the complex contains chemically and/or magnetically inequivalent phosphine ligands. It is therefore quite different from the cis isomer. However, like the latter species it has a singlet in its $^{31}P\{^1H\}$ spectrum while an *apparent* triplet is observed in the ^{31}P spectrum.

The X-ray structure determination of a crystal of *trans*-$[ReH_2(mhp)_2(PPh_3)_2]PF_6 \cdot C_2H_4Cl_2$ (**1**) was carried out at −62 °C. The structure refined without significant complication, although the crystal contained a disordered 1,2-dichloroethane molecule (for further details see the Experimental Section). The appropriate data are presented in Tables I, II, and VI and an ORTEP representation of the structure of the cation is given in Figure 3. Both **1** and **2** are clearly geometric isomers of the eight-coordinate complex $[ReH_2(mhp)_2(PPh_3)_2]PF_6$, and they preserve their separate identity *both in the solid state and in solution.* The P–Re–P angles in the structures of **1** and **2** are 168.76 (3) and 128.97 (6)°, respectively, a difference that is the origin of our designation of these two isomers as trans and cis, respectively.

Both isomers of $[ReH_2(mhp)_2(PPh_3)_2]PF_6$ share another property that is common to $[ReH_2(hp)_2(PPh_3)_2]PF_6$ and $[ReH_2(mp)_2(PPh_3)_2]PF_6$, namely, their ready deprotonation to the parent neutral monohydride. While both the cis and trans isomers of $[ReH_2(mhp)_2(PPh_3)_2]PF_6$ give the same product, the deprotonation of the former requires DBU, while either NEt_3 or DBU can be used to deprotonate *trans*-$[ReH_2(mhp)_2(PPh_3)_2]PF_6$.

Although solutions of both isomers are remarkably stable, we find that the trans isomer very slowly converts to the cis isomer. This was observed to occur in dichloromethane, 1,2-dichloroethane, and acetone although it doubtless also takes place in other solvents as well. A comparison was made of the trans → cis isomerization in CH_2Cl_2 at three temperatures (0, 20, and 40 °C). While no detectable amount (by $^{31}P\{^1H\}$ NMR) of the cis isomer had formed after four days at 0 °C, at 20 °C under these conditions the trans/cis isomer ratio was ca. 9/1. After four days at 40 °C, the cis isomer was now the dominant species, but a considerable quantity (ca. 30%) of the deprotonated complex $ReH(mhp)_2(PPh_3)_2$ had also formed under these conditions. At room temperature in dichloromethane the isomerization appears to be an intramolecular process that is independent of added ligand (in the form of PPh_3, Hmhp, or Limhp). It proceeds cleanly in an inert atmosphere with no observable side products, and can be followed by either ^{1}H or $^{31}P\{^1H\}$ NMR spectroscopy although the latter proved to be the most convenient. A CD_2Cl_2 solution of the trans isomer was sealed in an NMR tube (under a N_2 atmosphere) and the integrated intensity of the $^{31}P\{^1H\}$ signal was monitored over a period of several weeks to ca. 90% conversion. A CD_2Cl_2 solution of PPh_3 was used as an external standard. A zero-order rate constant, $k = (7.9 \pm 0.2) \times 10^{-9}$ M s^{-1} at 20 °C, was determined from the $^{31}P\{^1H\}$ NMR spectra. Further confirmation of the zero order was done by analysis of the rate of *appearance* of the cis isomer in the NMR experiment.

Discussion

The oxidation of $ReH(hp)_2(PPh_3)_2$ and $ReH(mp)_2(PPh_3)_2$ to their one-electron oxidized congeners, along with the previous report[8] of the oxidation of $ReH(mhp)_2(PPh_3)_2$ to $[ReH(mhp)_2(PPh_3)_2]PF_6$, provides a series of rare mononuclear paramagnetic rhenium(IV) hydrides that permits a detailed examination of the chemistry of this class of compound. While solutions of $[ReH(mp)_2(PPh_3)_2]PF_6$ are stable for prolonged periods, the corresponding hp- and mhp-containing salts decompose to give the dihydrido species $[ReH_2(hp)_2(PPh_3)_2]PF_6$ and *cis*-$[ReH_2(mhp)_2(PPh_3)_2]PF_6$, respectively, probably by a mechanism that involves some sort of disproportionation of the paramagnetic monohydrido cation $[ReH(L)_2(PPh_3)_2]^+$. In both reactions, small amounts of the rhenium(V) oxo complexes $[ReO(hp)_2(PPh_3)_2]PF_6$ and $[ReO(mhp)_2(PPh_3)_2]PF_6$ can also be isolated. These are probably formed as byproducts from the decomposition of that portion of the rhenium that must be sacrificed to provide the source of additional hydrogen necessary to convert $[ReH(L)_2(PPh_3)_2]^+$ to $[ReH_2(L)_2(PPh_3)_2]^+$. These oxo products do not appear to form from the isoelectronic species $[ReH_2(L)_2(PPh_3)_2]^+$ since deliberate attempts to convert *cis*-$[ReH_2(mhp)_2(PPh_3)_2]PF_6$ to $[ReO(mhp)_2(PPh_3)_2]PF_6$ upon its treatment with acid, small amounts of water, air, or oxygen at room temperature or under reflux were all unsuccessful. Even with the use of reaction times of several days, *cis*-$[ReH_2(mhp)_2(PPh_3)_2]PF_6$ failed to react in any way whatsoever. The source of oxygen for these oxo complexes remains unknown.

An X-ray structure determination on a crystal of $[ReO(mhp)_2(PPh_3)_2]PF_6 \cdot C_2H_4Cl_2$ shows it to be the first example[22,23]

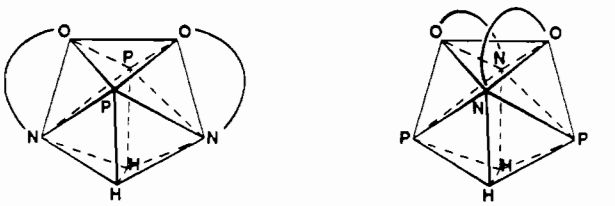

trans-$[ReH_2(mhp)_2(PPh_3)_2]PF_6$ *cis*-$[ReH_2(mhp)_2(PPh_3)_2]PF_6$

Figure 4. Idealized representation of the dodecahedral geometries of the cis and trans isomers of $[ReH_2(mhp)_2(PPh_3)_2]^+$.

of a structurally characterized seven-coordinate oxorhenium(V) complex (Figure 1). The structure can be best described as a distorted pentagonal bipyramid with the axial P(1)–Re–P(2) unit approaching linearity (this angle is 169.34 (8)°) and the two mhp ligands and oxo group forming the approximate pentagonal plane. Least-squares-planes calculations on the Re–O(10)–O(20)–N(21)–O(1)–N(11) plane show that the largest displacement of any of the six atoms that form the plane is 0.131 (1) Å for O(20). The Re atom is 0.001 (1) Å from this plane. The distance from P(1) to the least-squares plane is 2.495 (2) Å, while the distance from P(2) to the plane is 2.497 (3) Å. Within the pentagonal plane the five angles range from 59.8 (3) to 85.8 (3)°, reflecting both the small bite of the chelating mhp ligand and the bonding constraints engendered by the terminal Re=O bond whose length (1.692 (5) Å) is typical of that encountered in other oxorhenium(V) complexes.[22,23] Note that the geometry of the $OReN_2P_2$ fragment closely approaches that of a square pyramid, with the oxygen constituting the unique axial ligand atom.

The dihydrido complex *cis*-$[ReH_2(mhp)_2(PPh_3)_2]PF_6$ has properties that closely resemble those of its hp analogue (Table VII), and its crystal structure (Figure 2) confirms its eight-coordinate stereochemistry. What is remarkable is that this structure differs from that of the form of this complex (designated as the trans isomer) that is generated by the more logical synthetic strategy of protonating $ReH(mhp)_2(PPh_3)_2$ with HPF_6 (see Figure 3). Even more surprising is the discovery that these differences are retained in solution. This is the first time that such eight-coordinate geometric isomers have been structurally characterized.

Both structures (Figures 2 and 3) are based on dodecahedral geometries and each contains a pair of chelating mhp ligands, which in the trans isomer are approximately in the same plane. Least-squares planes calculations on the Re–O(12)–N(11)–O(22)–N(21) plane show that the largest displacement of any of the five atoms that form the plane is 0.068 (3) Å for O(22). A key difference between the structures of the two isomers is in the disposition of their hydride ligands. The two hydride ligands in the cis isomer form a plane with the rhenium center that is approximately perpendicular to the P–Re–P plane. In contrast, the hydride ligands in the trans isomer are approximately coplanar with the P–Re–P unit. Least-squares-planes calculations on the Re–P(1)–H(1)–P(2)–H(2) plane show that H(1) is 0.069 (42) Å and H(2) is 0.061 (47) Å from the plane. While significant distortions from an idealized dodecahedral geometry are present because of the disparate sets of ligands in the complexes, the hydrogen and oxygen atoms can be viewed as sitting at the A sites and the nitrogen and the phosphorus atoms at the B sites of an MA_4B_4 dodecahedron, as shown in Figure 4.[24]

These structural differences also accord with the NMR spectral properties of these two isomers (Figure S2). The observation of a binomial triplet for the hydride resonance of the cis isomer (δ +4.65, J_{P-H} = 46 Hz) is consistent with the expected magnetic and chemical equivalence of the phosphorus atoms, although it could also be characteristic of a fluxional molecule. In the case of the trans isomer, the resonance for the two chemically equivalent hydride ligands (δ +6.66) has the appearance of a doublet of doublets. Analysis and simulation of this resonance as a AA'XX' pattern yields four coupling constants: $^2J_{P-H}$ = 54.0 Hz, $^2J_{P'-H}$ = 6.0 Hz, $^2J_{H-H}$ = 7.7 Hz, and $^2J_{P-P}$ = 104.0 Hz. With this set of parameters the ^{31}P NMR spectrum, which has the appearance of an apparent triplet, can be simulated very well.[25]

On the basis of the crystallographic results and ^1H NMR spectral data, both isomers appear to be classical dihydrides. The H–H distances of 1.53 (5) Å for **1** and 1.6 (1) Å for **2**, as well as the H–Re–H angles of 56 (2)° for **1** and 61 (3)° for **2**, are normal for classical hydrides.[26] Over the temperature range of +25 to −80 °C the Re–*H* resonances remained essentially unchanged, except for a slight broadening and a small upfield shifting of the signals by between 0.2 and 0.4 ppm at the lower temperature limit. The ^1H NMR spectrum of the *trans*-$[ReHD(mhp)_2(PPh_3)_2]^+$ cation, which can be generated by the addition of a 10-fold excess of CF_3CO_2D to a CD_2Cl_2 solution of $ReH(mhp)_2(PPh_3)_2$ in a sealed NMR tube under N_2 gas, shows a hydride resonance that has shifted approximately 0.1 ppm downfield from that of the dihydride complex. As expected, the hydride–deuteride complex does not exhibit H–D coupling, which would be characteristic of η^2-HD bonding.[27]

The very slow conversion of the trans isomer to the cis which can take place in solvents such as dichloromethane poses something of a puzzle since it appears to be zero order (k_{obs} = (7.9 ± 0.2) × 10^{-9} M s^{-1} at 20 °C). This reaction order is not readily explained since a simple intramolecular isomerization would be expected to be first order. We have established that the reaction is not affected by light, the presence of acid (from added HPF_6), or small amounts of water, nor is it affected as far as we can tell by the surface of the borosilicate glass vessel used. While this isomerization process is not fully understood, the data support the trans isomer as being the kinetic product of the protonation of $ReH(mhp)_2(PPh_3)_2$.

A possible explanation for the remarkable stability of the trans isomer is that the mhp ligands, which lie essentially in a plane with their methyl groups projecting toward each other (Figure 3), provide a barrier to the rotation of the ReH_2 unit that may be necessary to convert it to the more thermodynamically favored cis isomer. This process can only be accomplished by a concomitant twisting of the mhp ligands from this planar arrangement, a process that is apparently not very energetically favorable. In support of this contention is our observation that the analogous complexes with ligands that do *not* contain methyl groups, i.e., $[ReH_2(L)_2(PPh_3)_2]PF_6$, where L is hp or mp, appear to exist exclusively in the cis form or are fluxional molecules that do not exhibit geometric isomerism.

Acknowledgment. Support from the National Science Foundation, through Grant No. CHE88-07444 to R.A.W. and Grant. No. CHE86-15556 for the purchase of the microVAX II computer and diffractometer, is gratefully acknowledged. We also acknowledge the National Institutes of Health (Grant No. RR-01077) and the National Science Foundation (Grant No. 8714258) for funds for the purchase of the NMR spectrometers and Debra W. Johnson for assistance with the kinetic experiments.

(22) Conner, K. A.; Walton, R. A. In *Comprehensive Coordination Chemistry*; Wilkinson, G., Ed.; Pergamon: Oxford, England, 1987; Chapter 43, pp 177–185.

(23) Nugent, W. A.; Mayer, J. M. *Metal-Ligand Multiple Bonds*; J. Wiley & Sons: New York, 1988, pp 175 and 176.

(24) Kepert, D. L. In *Comprehensive Coordination Chemistry*; Wilkinson, G., Ed.; Pergamon: Oxford, England, 1987; Chapter 2, p 84.

(25) The simulated spectra were obtained using the program RACCOON by P. Schatz, University of Wisconsin, Madison, WI, Project SERAPHIM, IB 003.

(26) In addition, T_1 measurements for both isomers are consistent with this conclusion. For the trans isomer, the observed T_1(min) (at 200 MHz) was 52 ± 11 ms (measured at −76 °C), and for the cis isomer, the observed T_1(min) (at 200 MHz) was 59 ± 7 ms (measured at −74 °C). For a recent discussion of the T_1 method, see: Crabtree, R. H.; Luo, X. *Inorg. Chem.* **1990**, *29*, 2788.

(27) For data on a similar shift in a hydride resonance, see: Chinn, M. S.; Heinekey, D. M.; Payne, N. G.; Sofield, C. D. *Organometallics* **1989**, *8*, 1824.

Supplementary Material Available: Tables giving full details of the crystal data and data collection parameters for **1–4** (Tables S1–S4), positional parameters for all atoms (Tables S5–S8), anisotropic thermal parameters (Tables S9–S12), and complete bond distances (Tables S13–S16) and bond angles (Tables S17–S20) and figures showing the structure and atomic numbering scheme for the cation of **3** (Figure S1) and the ^{1}H NMR spectra of the trans and cis isomers of $[ReH_2(mhp)_2(PPh_3)_2]PF_6$ (Figure S2) (78 pages); tables of observed and calculated structure factors (136 pages). Ordering information is given on any current masthead page.

Contribution from the Department of Chemistry, University of Utah, Salt Lake City, Utah 84112

Synthesis, Structure, and Reactivity of Chiral Rhenium Amine Complexes of the Formula $[(\eta^5\text{-}C_5H_5)Re(NO)(PPh_3)(NRR'R'')]^+TfO^-$

Michael A. Dewey, D. Andrew Knight, Darryl P. Klein, Atta M. Arif, and J. A. Gladysz*

Received July 19, 1991

Reactions of $(\eta^5\text{-}C_5H_5)Re(NO)(PPh_3)(OTf)$ (**2**) and (**a**) ammonia, (**b**) methylamine, (**c**) [(trimethylsilyl)methyl]amine, (**d**) aniline, (**e**) isopropylamine, (**f**) dimethylamine, (**g**) dibenzylamine, (**h**) pyrrolidine, and (**i**) trimethylamine give amine complexes $[(\eta^5\text{-}C_5H_5)Re(NO)(PPh_3)(NRR'R'')]^+TfO^-$ (**3**, 55–99%). An analogous reaction of optically active (+)-(*R*)-**2** and methylamine gives (+)-(*S*)-**3b** (79%, >98% ee, retention of configuration). The spectroscopic properties of **3a–i** and isotopomer **3a**-$^{15}NH_3$ are studied in detail. The crystal structure of **3f** (monoclinic, $P2_1/n$, a = 13.925 (2) Å, b = 24.467 (3) Å, c = 8.148 (1) Å, β = 93.398 (4)°, Z = 4) shows P–Re–N–H and ON–Re–N–H torsion angles of −52 and 40°, and a N···H···OTf hydrogen bond (H···O 2.37 (5) Å). Reactions of **3a,b,f** with $(CH_3CH_2)_4N^+CN^-$ and $PPN^+N_3^-$ (PPN = $Ph_3P{=}N{=}PPh_3$) give the substitution products $(\eta^5\text{-}C_5H_5)Re(NO)(PPh_3)(CN)$ (**4**, 86–94%) and $(\eta^5\text{-}C_5H_5)Re(NO)(PPh_3)(N_3)$ (**5**, 61–98%). Reaction of $(\eta^5\text{-}C_5H_5)Re(NO)(PPh_3)(CH_3)$ with $HBF_4{\cdot}OEt_2$ and then $PPN^+N_3^-$ in chlorobenzene also gives **5** (67%). Reaction of (+)-(*S*)-**3b** and $(CH_3CH_2)_4N^+CN^-$ gives (+)-(*S*)-**4** (>98% ee, retention of configuration).

Amines are probably the most widespread σ donor ligands in inorganic coordination compounds, and also occur frequently in organometallic complexes.[1] Further, many biological molecules contain amine functional groups. These can bind to metals in both enzymes and purely synthetic molecules.[2] Metal amine complexes have also received attention as reactivity models for catalytic hydrodenitrogenation (HDN),[3] and their physical properties have been the subject of detailed studies.[4]

The readily available chiral rhenium fragment $[(\eta^5\text{-}C_5H_5)Re(NO)(PPh_3)]^+$ (I) forms adducts with a variety of σ- and π-donor ligands.[5,6] We have studied the chemical and physical properties of the resulting complexes in detail. Many highly diastereoselective reactions have been found which entail formal transfer of the rhenium-centered chirality to a new ligand-based chiral center.[7] As a preface to investigations involving unsaturated nitrogen-containing ligands, we sought to define preparative routes to amine complexes, as well as basic spectroscopic, structural, and chemical properties.

Scheme I. Synthesis of Amine Complexes $[(\eta^5\text{-}C_5H_5)Re(NO)(PPh_3)(NRR'R'')]^+TfO^-$ (**3**)

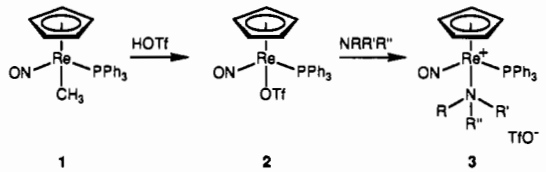

a, R = R' = R'' = H
b, R = R' = H, R'' = CH_3
c, R = R' = H, R'' = $CH_2Si(CH_3)_3$
d, R = R' = H, R'' = C_6H_5
e, R = R' = H, R'' = $CH(CH_3)_2$
f, R = H, R' = R'' = CH_3
g, R = H, R' = R'' = $CH_2C_6H_5$
h, R = H, R', R'' = CH_2CH_2-)$_2$
i, R = R' = R'' = CH_3

In this paper, we report (1) high-yield syntheses of racemic and optically active chiral amine complexes of the formula $[(\eta^5\text{-}C_5H_5)Re(NO)(PPh_3)(NRR'R'')]^+ TfO^-$, (2) a thorough characterization of their spectroscopic properties, (3) a crystal structure of a representative complex, and (4) substitution reactions of selected compounds. A portion of this work has been communicated.[8]

Results

1. Synthesis and Spectroscopic Characterization of Amine Complexes. The methyl complex $(\eta^5\text{-}C_5H_5)Re(NO)(PPh_3)(CH_3)$ (**1**)[9] and triflic acid (HOTf) were reacted at −45 °C in toluene to generate the triflate complex $(\eta^5\text{-}C_5H_5)Re(NO)(PPh_3)(OTf)$ (**2**).[10] Then excesses of (**a**) ammonia, (**b**) methylamine, (**c**) [(trimethylsilyl)methyl]amine, (**d**) aniline, (**e**) isopropylamine, (**f**) dimethylamine, (**g**) dibenzylamine, (**h**) pyrrolidine, and (**i**) trimethylamine were added, as shown in Scheme I. The resulting

(1) House, D. A. In *Comprehensive Coordination Chemistry*; Wilkinson, G., Gilliard, R. D., McCleverty, J. A., Eds.; Pergamon: New York, 1987; Vol. 2, Chapter 13.1.
(2) See, for example, the following references. (a) Amino sugars: Yano, S. *Coord. Chem. Rev.* **1988**, *92*, 113. (b) Amino acids: Zahn, I.; Wagner, K. P.; Beck, W. *J. Organomet. Chem.* **1990**, *394*, 601 and references therein. (c) Adenine–uracil base pairs: Ghose, R. *Inorg. Chim. Acta* **1989**, *156*, 303. (d) Roundhill, D. M. Submitted for publication in *Chem. Rev.*
(3) (a) Laine, R. M. *New J. Chem.* **1987**, *11*, 543 and references therein. (b) Fish, R. H.; Baralt, E.; Kim, H.-S. *Organometallics* **1991**, *10*, 1965 and references therein.
(4) See, for example: (a) Burkey, T. J. *Polyhedron* **1989**, *8*, 2681. (b) Trogler, W. C.; Seligson, A. L. *J. Am. Chem. Soc.* **1991**, *113*, 2520.
(5) (a) Fernández, J. M.; Gladysz, J. A. *Organometallics* **1989**, *8*, 207. (b) Kowalczyk, J. J.; Agbossou, S. K.; Gladysz, J. A. *J. Organomet. Chem.* **1990**, *397*, 333.
(6) Some recent references: (a) Buhro, W. E.; Zwick, B. D.; Georgiou, S.; Hutchinson, J. P.; Gladysz, J. A. *J. Am. Chem. Soc.* **1988**, *110*, 2427. (b) Winter, C. H.; Veal, W. R.; Garner, C. M.; Arif, A. M.; Gladysz, J. A. *Ibid.* **1989**, *111*, 4766. (c) Bodner, G. S.; Peng, T.-S.; Arif, A. M.; Gladysz, J. A. *Organometallics* **1990**, *9*, 1191. (d) Agbossou, S. K.; Smith, W. W.; Gladysz, J. A. *Chem. Ber.* **1990**, *123*, 1293. (e) Kowalczyk, J. J.; Arif, A. M.; Gladysz, J. A. *Organometallics* **1991**, *10*, 1079. (f) Quirós Méndez, N.; Arif, A. M.; Gladysz, J. A. *Ibid.* **1991**, *10*, 2199.
(7) Representative examples: (a) Garner, C. M.; Quirós Méndez, N.; Kowalczyk, J. J.; Fernández, J. M.; Emerson, K.; Larsen, R. D.; Gladysz, J. A. *J. Am. Chem. Soc.* **1990**, *112*, 5146. (b) Peng, T.-S.; Gladysz, J. A. *Tetrahedron Lett.* **1990**, *31*, 4417. (c) Crocco, G. L.; Lee, K. E.; Gladysz, J. A. *Organometallics* **1990**, *9*, 2819. (d) Dalton, D. M.; Fernández, J. M.; Emerson, K.; Larsen, R. D.; Arif, A. M.; Gladysz, J. A. *J. Am. Chem. Soc.* **1990**, *112*, 9198. (e) Dalton, D. M.; Garner, C. M.; Fernández, J. M.; Gladysz, J. A. *J. Org. Chem.* **1991**, *56*, 6823.
(8) Dewey, M. A.; Bakke, J. M.; Gladysz, J. A. *Organometallics* **1990**, *9*, 1349.
(9) Tam, W.; Lin, G.-Y.; Wong, W.-K.; Kiel, W. A.; Wong, V. K.; Gladysz, J. A. *J. Am. Chem. Soc.* **1982**, *104*, 141.
(10) (a) Merrifield, J. H.; Fernández, J. M.; Buhro, W E.; Gladysz, J. A. *Inorg. Chem.* **1984**, *23*, 4022. (b) OTf = OSO_2CF_3.

0020-1669/91/1330-4995$02.50/0